Proceedings of the 2006 IASME/WSEAS International Conference on Continuum Mechanics, Chalkida, Greece, May 11-13, 2006 (pp44-48)

The effect of cold rolling on the creep behavior of Udimet 188

Carl Boehlert
Department of Chemical Engineering and Materials Science
Michigan State University
East Lansing, MI 48824
U.S.A.

Abstract: - A Udimet 188 alloy was subjected to thermo-mechanical processing in attempt to understand the effects of cold-rolling deformation on the creep behavior. Commercially available sheet was cold rolled to either 10%, 25%, or 35% deformation followed by a solution treatment at 1191°C for one hour followed by air cooling. This sequence was repeated four times and the resultant microstructure was characterized using Electron Backscattered Diffraction (EBSD). In addition, the effect of cold rolling on the high-temperature (650-815°C) creep behavior was evaluated. Conventional lever-arm creep experiments were performed in an open air environment and novel *in-situ* creep experiments were performed inside an SEM chamber. The measured creep stress exponents suggested that dislocation creep was dominant at 760°C for stresses ranging between 100-220MPa. The measured activation energies (402-450kJ/mol) suggested that lattice self diffusion was dominant; however the material was susceptible to grain boundary cracking during creep deformation. EBSD, performed both prior to and after creep testing, indicated that high-angle grain boundaries were more susceptible to cracking than low angle grain boundaries and coincident site lattice boundaries. This result has significant implications regarding grain boundary engineering of this alloy.

Key-Words: - Cobalt-based alloy, Electron backscattered diffraction, Creep deformation, Microstructure,

1 Inroduction

Udimet alloy 188 is a cobalt-nickel-chromium-tungsten commercially available alloy with good creep strength and oxidation resistance up to 1093°C. The high chromium content along with a small amount of lanthanum produces a corrosion resistant scale. The alloy also has exhibited good fabricability, tensile ductility, weldability, low-cycle fatigue, and oxidation resistance [1-3]. It has useful applications in gas turbines, combustors, flame holders, liners, and transition ducts. However, a complete understanding of the physical mechanisms responsible for the elevated-temperature creep behavior and associated microstructure-property relationships in Udimet alloy 188 is lacking. In particular, it has yet to be established if this alloy can be thermomechanically processed to significantly alter the grain boundary character distribution (GBCD), which has proven to have a significant influence on the mechanical deformation behavior of other fcc-based superalloy systems [4-17]. The process of altering the GBCD through processing is called grain boundary engineering (GBE) and is traced back to the work of Watanabe [18]. GBCD refers to the number of each type of boundary (high-angle boundary (greater than 15° misorientation), low-angle boundary (less than 15° misorientation), and coincident site lattice boundary (where the reciprocal of the number of coincident sites is noted; for example a twin boundary has three coincident sites as is denoted as Σ3) found in a microstructure and implicitly relates to the spatial configuration of these boundaries, i.e., nature of the boundary network and various types of boundary junctions. Previous data has suggested that a high fraction of low-angle and coincident site lattice boundaries significantly enhances resistance to creep and grain boundary sliding at elevated temperature [17].

This work was intended to evaluate processing-microstructure-property relationships of Udimet 188. In particular the effect of cold rolling on the microstructure and high-temperature creep behavior was evaluated.

2 Experimental

The as-received Udimet 188 material was subjected to the following strain annealing sequence: cold rolled to either 10%, 25%, or 35% deformation followed by a solution treatment at 1191°C for one hour followed by air cooling. This sequence was repeated four times. It is note that the final thickness of the 35% cold rolled sheet was 0.xxthat of the 10% cold rolled sheet, and the final thickness of the 25% cold rolled sheet was 0.xx that of the 10% cold rolled sheet.

Each processed sheet was sectioned and metallographically polished to prepare it for imaging. Spatially resolved EBSD orientation maps were obtained from polished sections using a Field Emission Gun CAMSCAN 44FE scanning electron microscope (SEM). The EBSD hardware and software were manufactured by

EDAX-TSL, Inc. The specimens were ground mechanically by 15μm, 6μm and 1μm diamond suspension for 10 minutes respectively, and then polished by 0.06μm colloidal silica for 60 minutes. The typical step size used to obtain the EBSD orientation maps was 2μm and in most cases over 500 grains were analyzed.

Blanks from the thermomechanically processed (TMP) sheet materials were machined, using either electrodischarge machining or milling, into a flat dogbone geometry used for tensile-creep specimens. Open-air creep experiments were performed on a vertical Applied Test System, Incorporated load frame with a 20:1 lever-arm ratio. The testing temperatures and stresses ranged between 760-815°C and 100-220MPa, respectfully. Although the experiments were constant load, in most cases the reduction in cross-sectional area was not sufficient to significantly alter the stress. Therefore the stresses were assumed to be constant. Specimen temperatures were monitored by three chromel-alumel type K thermocouples located within the specimen's reduced section. Targeted temperatures were maintained within ± 2°C. All creep specimens were loaded parallel to the rolling direction, and the experiments were conducted such that the specimens were soaked at the creep temperature for at least one hour prior to applying load in order to minimize the thermal stresses. After the creep strain had proceeded well into the secondary regime, either the load or temperature was changed or the creep test was discontinued. The tested specimens were cooled under load to minimize recovery of the deformed structures. In addition, a miniature dogbone geometry was used for evaluating the creep deformation behavior *in-situ* where the creep deformation was recorded at certain creep strain levels using SEM imaging. In this technique a specially designed tensile stage (designed by Ernest Fullam, Inc. Latham, NY, USA), equipped with a tungsten-based heating system, was utilized. The sample was imaged in backscatter electron (BSE) mode both prior to and after creep deformation. The applied stresses ranged between 300-350MPa and the temperature was 650^{o}C for these experiments. In addition, EBSD orientation maps were acquired both prior to and after deformation.

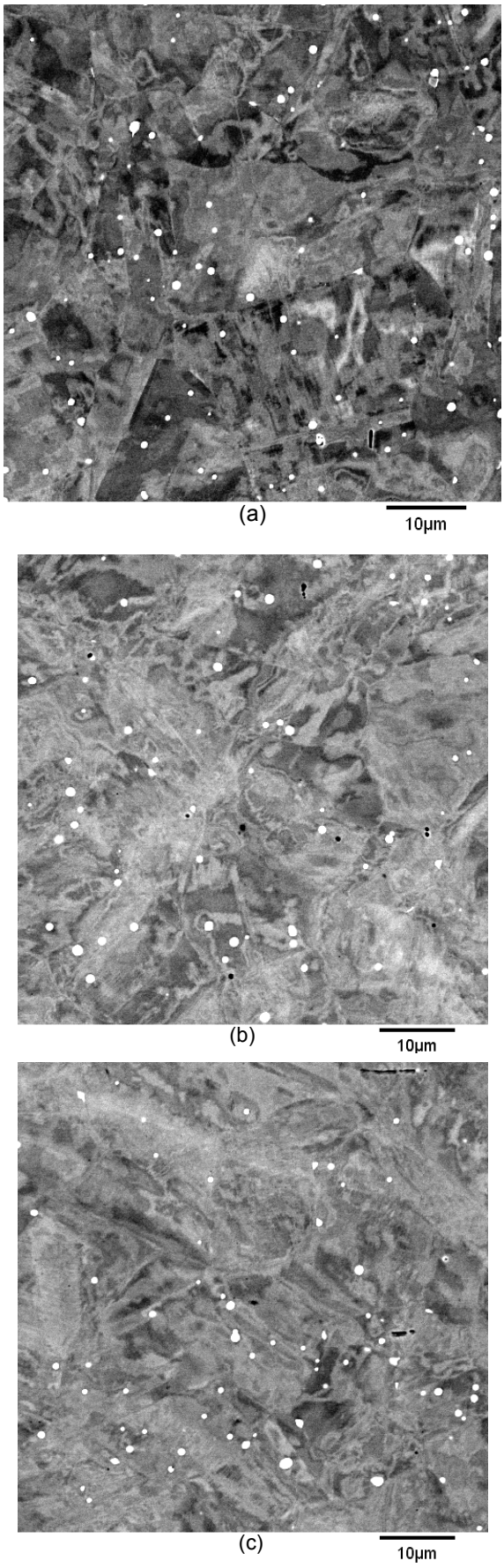

Fig. 1. BSE SEM micrographs of the (a) 10%, (b) 25%, and (c) 35% cold rolled microstructures.

3 Results and Discussion

3.1 Microstructure

Table I lists the measured alloy composition. Fig. 1 illustrates BSE SEM images of the thermomechanically processed microstructures. Each microstructure exhibited approximately two volume percent of fine equiaxed precipitates (white particles in the images) homogeneously distributed throughout the equiaxed fcc grains as well as at their grain boundaries. The average

Table I. Measured Composition of the Udimet 188 alloy in wt.%

Co	Ni	Cr	W	Fe	Mn	Si	C	La	B
39	22.0	22.0	14.0	3.0	1.25	0.35	0.10	0.03	0.015

equiaxed fcc grain size ranged from 12-16μm depending on the amount of cold rolling. Fig. 2 illustrates representative EBSD data including an orientation map (Fig. 2a) of a 10% cold rolled microstructure. The orientation map shows that the alloy exhibited an equiaxed microstructure and the orientations were distributed fairly evenly. Pole figure analysis indicated that the microstructure was not strongly textured. The GBCD was characterized using orientation maps to determine the orientation relationships between grains. A significant volume fraction of twins (up to 0.4) were observed in this microstructure (Fig. 2b). It is noted that the grain boundaries were intact and no cracks were present in any of the thermomechanically-processed microstructures.

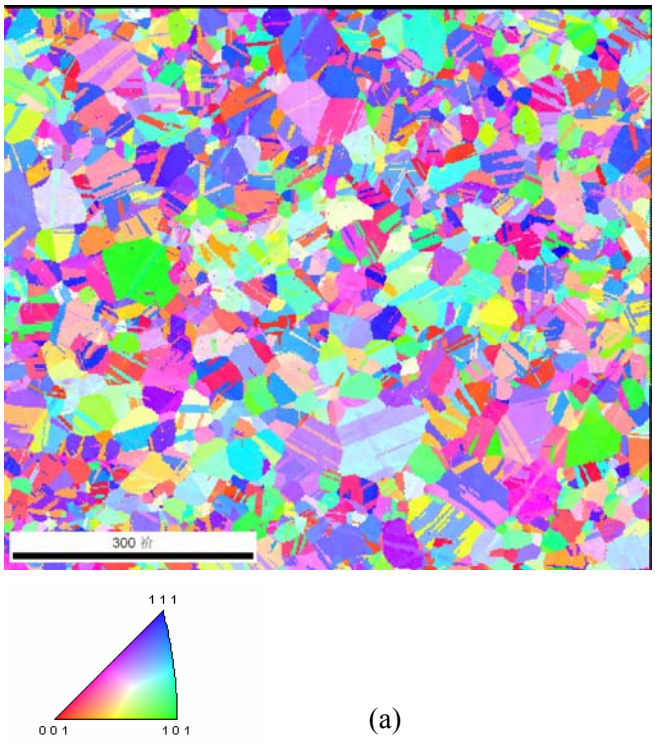

(a)

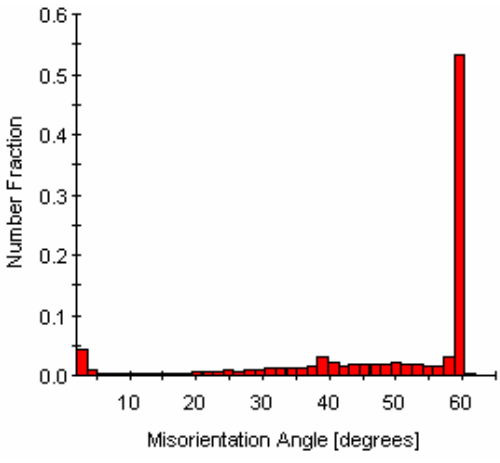

(b)

Fig. 2. (a) EBSD orientation map and (b) grain boundary misorientation angle chart for a 10% CR microstructure.

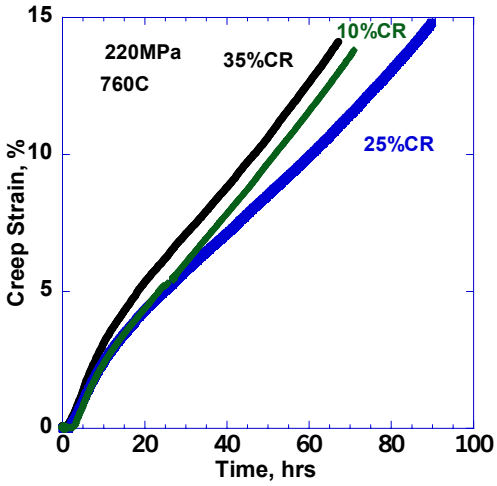

Fig. 3. Creep strain versus time plots for the three TMP conditions at T=760°C and σ=220MPa.

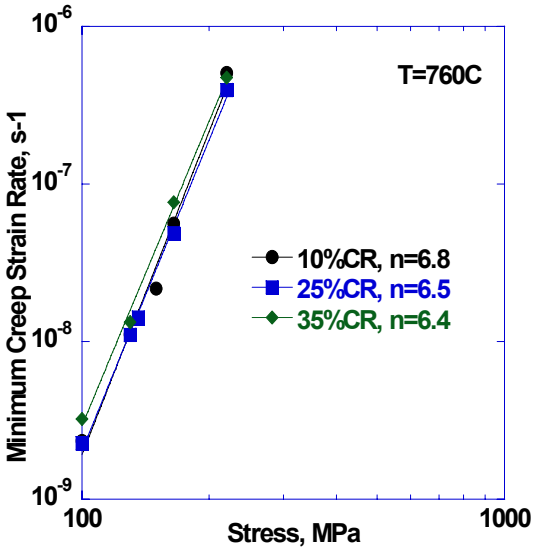

(a)

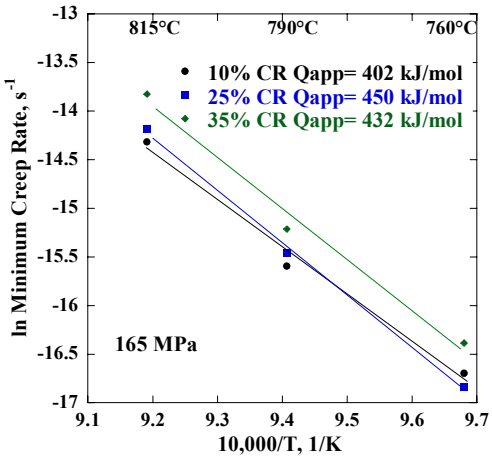

(b)

Fig. 4. (a) Minimum creep rate versus applied stress and (b) ln minimum creep rate versus 1/T for the three cold rolled conditions.

Table II Creep Exponents and Activation Energies

CR, %	σ/T, MPa/°C	n	σ/T, MPa/°C	Qapp, kJ/mol
10%	100-220/760	6.8	165/760-815	402
25%	100-220/760	6.5	165/760-815	450
35%	100-220/760	6.4	165/760-815	432

4 Summary and Conclusions

This work evaluated the effect of cold rolling deformation on the microstructure and creep behavior of Udimet 188 alloy. The 10% and 25%CR material exhibited lower strain rates that the 35%CR material. Thus more than 25% cold rolling degrades the creep resistance of Udimet 188. For the applied stresses and temperature evaluated, the measured creep parameters suggested that dislocation creep was the dominant deformation mechanism. Independent of the extent of cold rolling deformation, the material was susceptible to grain boundary cracking during creep deformation, where EBSD, performed both prior to and after creep testing, indicated that high-angle grain boundaries were more susceptible to cracks than low angle grain boundaries and coincident site lattice boundaries.

Acknowledgments

This work was supported by the National Science Foundation through grant DMR-0533954. The author is grateful to Mr. Nathan Eisinger (Special Metals Corporation) for performing the alloy processing and Mr. Adam King (formerly at Michigan State University and now at Rocketdyne) for assistance with the mechanical testing.

References:

[1] C.J. Lissenden, J.F. Colaiuta, B.A. Lerch, Hardening behavior of three metallic alloys under combined stress at elevated temperature, Acta Mechanica, Vol. 169, 2004, pp. 53-77.

[2] D. Zhu, D.S. Fox, R.A. Miller, Oxidation and Creep-Enhanced Fatigue of Haynes 188 Alloy-Oxide Scale System Under Simulated Pulse Detonation Engine Conditions, Ceramic Engineering and Science Proceedings, Vol. 23.4, 2002, pp. 547-53.

[3] J. Chen, P.K. Laiw, et al., Tensile Hold Low-Cycle Fatigue Behavior of Cobalt-Based Haynes 188 Superalloy, Scripta Materialia, Vol. 44, 2001, pp. 859-865.

[4] G. Palumbo, Metal alloys having improved resistance to intergranular stress corrosion cracking. U.S. Patent 5,817,193, 1998.

[5] M. Kumar, W.E. King, A.J. Schwartz, Modifications in the microstructural topology in FCC materials with thermomechanical processing, Acta Materialia, Vol. 48, 2000, p. 2081.

[6] E.M. Lehockey, G. Palumbo, P. Lin, Improving the Weldability and Service Performance of Nickel- and Iron-Based Suparalloys by Grain boundary Engineering, Metallurgical and Materials Transactions, Vol. 29A 1998, pp. 3069-79.

[7] B. Alexandreanu, B.M. Capell, G. Was, Combined effect of special grain boundaries and grain boundary carbides on IGSCC, Materials Science and Engineering, Vol. 300A, 2001, pp. 94-104.

[8] E.M. Lehockey, G. Palumbo, P. Lin, A.M. Brennenstuhl, On the Relationship Between Grain boundary Character Distribution and Intergranular Corrosion, Scripta Materialia, Vol. 36, No. 10, 1997, pp. 1211-18.

[9] C. Cheung, U. Erb, G. Palumbo, Applications of Grain Boundary Engineering Concepts to Alleviate Intergranular Cracking in Alloys 600 and 690, Materials Science and Engineering, Vol. 185A, 1994, pp. 39-43.

[10] D. Crawford, The Effect of Grain boundary Misorientation on the Intergranular Cracking Behavior of Ni-16Cr-9Fe in 360°C Argon and High Purity Water, PhD. Thesis, University of Michigan, 1991.

[11] G. Palumbo, K.T. Aust, Special Properties of Σ Grain Boundaries, Materials Interfaces: Atomic Level Structure and Properties, eds. D. Wolf, and S. Yip, Chapman and Hall NY, 1989, pp. 190-211.

[12] G. Palumbo, E.M. Lehockey, P. Lin, Applications for Grain Boundary Engineered Materials, Journal of Metals, February 1998, pp. 40-43.

[13] P. Lin, G. Palumbo, U. Erb, K.T. Aust, Influence of Grain Boundary Character Distribution on Sensitization and Intergranular Corrosion of Alloy 600, Scripta Materialia, Vol. 33, No. 9, 1995, pp. 1387-92.

[14] G.S. Was, V. Thaveeprungsriporn, D.C. Crawford, Grain Boundary Misorientation Effects on Creep and Cracking in Ni-Based Alloys, Journal of Metals, February 1998, 44-49.

[15] V. Thaveeprungsriporn, G. Was, The Role of Coincidence-Site-Lattice Boundaries in Creep of Ni-16Cr-9Fe at 360°C, Metallurgical and Materials Transactions, Vol. 28A, 1997, pp. 2101-2112.

[16] G. Palumbo and K.T. Aust, "Structure-Dependence of Intergranular Corrosion in High Purity Nickel", Acta. Metall. Mater., Vol. 38, no. 11, 1990, pp. 2343-2352.

[17] E.M. Lehockey, G. Palumbo, On the creep behavior of grain boundary engineered nickel, Materials Science and Engineering, Vol. A237, 1997, pp. 168–172.

[18] T. Watanabe, An approach to grain boundary design for strong and ductile for strong and ductile polycrystals, Res Mechanics, Vol. 11, 1984, pp. 47-84.

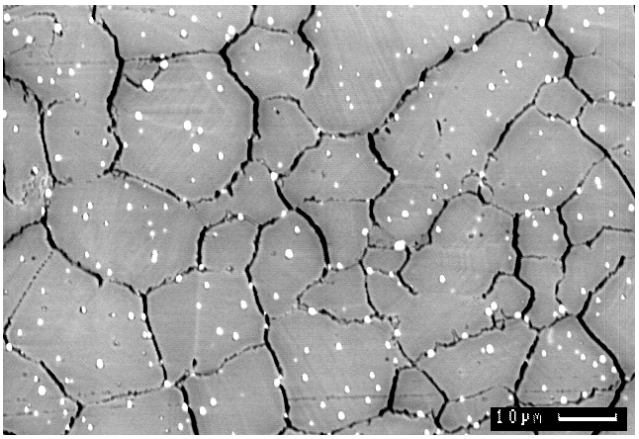

(a)

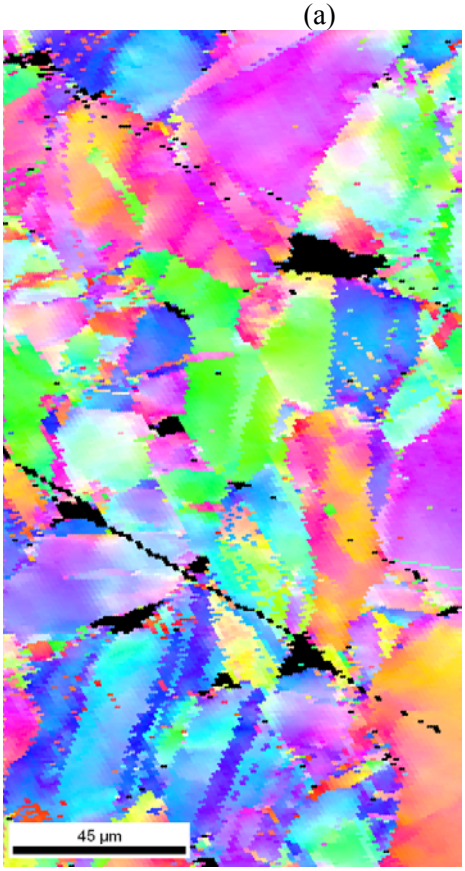

(b)

Figure 5. (a) BSE SEM image of a 25% cold rolled sample that was tested *in-situ* at 650C and 300MPa and (b) a EBSD map of a 25% cold rolled sample that had undergone a creep rupture experiment at 815C and 165MPa and exhibited over 20% strain to failure